ISSN 2176-5480

22nd International Congress of Mechanical Engineering (COBEM 2013)
November 3-7, 2013, Ribeirão Preto, SP, Brazil

A NEW PERSPECTIVE ON THE INTERNAL HEAT EXCHANGE IN THE VAPOR COMPRESSION CYCLE

Christian J. L. Hermes, chermes@ufpr.br
Laboratory of Thermodynamics and Thermophysics, Department of Mechanical Engineering, Federal University of Paraná
81531990 Curitiba-PR, Brazil

Abstract. *This paper comes up with a new perspective on the effects of the internal heat exchanger on the thermodynamic performance of vapor compression refrigeration systems. The thermodynamic exercise was carried out for refrigerants R134a, R22, R290, R600a and R717, assuming the cooling capacity is constrained whereas the working pressures are free to float. It is shown that the coefficient of performance of the refrigeration cycle may increase or decrease depending not only on the refrigerant properties, but also on the change experienced by the evaporating pressure. A thermodynamic criterion to predict whether or not the COP will improve is also reported.*

Keywords: *vapor-compression refrigeration, internal heat exchanger, thermodynamic analysis*

1. INTRODUCTION

Internal heat exchangers (IHX), also known as liquid-vapor and liquid-to-suction heat exchangers, are employed in refrigeration cycles, as depicted in Fig. 1, not only to reduce the vapor quality of the refrigerant entering the evaporator, thus increasing the specific refrigerating effect, but also to avoid the entrance of liquid into the compressor and the frost buildup over the suction line. From the classical refrigeration textbooks (Gosney, 1982; Stoecker and Jones, 1982), it is well-known that the IHXs might either improve or worsen the system coefficient of performance, COP, which is defined as the ratio between the cooling capacity and the compression work.

Domanski et al. (1994) studied the thermodynamic conditions required for performance improvement in cases where the working pressures of the standard and the modified cycle (i.e. the one with the iHX) are the same, so that the cooling capacity is free to float. For this purpose, they derived a concise mathematical formulation which expresses the ratio between the coefficient of performance of the cycle using an internal heat exchanger and the COP of the standard refrigeration cycle as a function of the temperature lift and the suction line superheating, and concluded that the COP and the volumetric refrigerating capacity of the modified cycle experience the same variation in comparison to the standard one. Klein et al. (2000) noticed that the adoption of an internal heat exchanger reduces the refrigerant mass flow rate as compressors are fixed volumetric flow devices. They gathered data from numerical calculations carried out for several refrigerants and refrigerant mixtures, and concluded that the relative capacity variation due to the internal heat exchanger is more significant for high temperature lifts and working fluids having a relatively small value of $h_{lv,e}/c_{pl,e}t_{cr}$, a dimensionless quantity introduced by the authors.

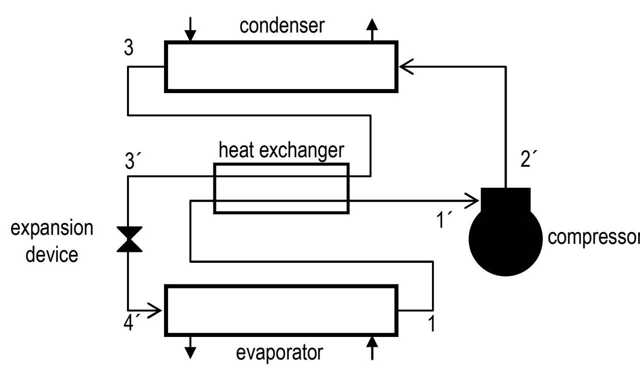

Figure 1. Schematic of the refrigeration cycle employing an internal heat exchanger

Nonetheless, in real applications, the refrigeration system is designed to accomplish a certain cooling capacity. Therefore, a more realistic analysis lies in maintaining the cooling capacity constrained, whereas the working pressures are free to float. The constrained conditions of the previous thermodynamic analyses (i.e. constrained pressures) as well as the lack of generality of the sophisticated (non-equilibrium) system simulation models have motivated the present work, which is aimed at evaluating, by means of a purely thermodynamic exercise (i.e. without requiring any component-level information in addition to the internal heat exchanger effectiveness), the effects of the internal heat exchange on the system COP in cases when the cooling capacity is constrained.

2. CONSTRAINED PRESSURES

This exercise starts with the textbook approach (Gosney, 1982; Stoecker and Jones, 1982), according to which the working pressures are kept constrained. The comparison between the standard (points 1-2-3-4 in Fig. 2) and the modified cycle (points 1′-2′-3′-4′ in Fig. 2) assumes that both run with the same compressor, i.e. $\dot{V} = \dot{V}'$, where the superscript ′ stands for the modified refrigeration cycle.

Thus, the volumic refrigerating effect produced and the mean effective pressure (i.e., compression work per unit volume) required by the standard cycle are respectively calculated from:

$$q_v = \eta_v \frac{h_1 - h_3}{v_1} \tag{1}$$

$$w_v = \eta_v p_e Y \tag{2}$$

where $h_1 - h_3$ is the specific refrigerating effect, v_1 is the specific volume ate the compressor inlet, $\eta_v = 1 - c\left(r^{1/k} - 1\right)$ is the volumetric efficiency of the compressor, $r = p_c/p_e$ is the pressure ratio, c is the compressor clearance, $k = c_p/c_v$ is the isentropic exponent, and $Y = \frac{k}{k-1}\left(r^{\frac{k-1}{k}} - 1\right)$ for $k \neq 1$. The COP of the standard refrigerating cycle is calculated from:

$$COP = \frac{q_v}{w_v} = \frac{h_1 - h_3}{v_1 p_e Y} \tag{3}$$

Similarly, the COP of the modified cycle is calculated from:

$$COP' = \frac{h_g' - h_3'}{v_1' p_e' Y'} \tag{4}$$

where $h_3' = h_1 - h_1' + h_3$ is yielded from an energy balance in the internal heat exchanger, whereas the refrigerant condition at the compressor entrance (point 1′) is obtained from the definition of heat exchanger effectiveness, ε, so that $t_1' = t_e + \varepsilon(t_c - t_e)$. The comparison criterion, as proposed by Domanski et al. (1994), is obtained by dividing eq. (4) by eq. (3). Also, assuming that $p_c' = p_c$, $p_e' = p_e$, it follows that $h_g' = h_g = h_1$, $\eta_v = \eta_v'$, and $Y = Y'$, thus yielding

$$\frac{COP'}{COP} = \frac{h_1 - h_3'}{h_1 - h_3}\frac{v_1}{v_1'} = \frac{q_v'}{q_v} \tag{5}$$

Equation (5) shows that the COP and the volumetric capacity experience the same variation in case an internal heat exchanger is adopted. Representing the specific volume as a function of refrigerant pressure and temperature, v=v(t,p),

$$\frac{dv}{v} = \beta dt - \alpha dp \tag{6}$$

where $\beta = (1/v)(\partial v/\partial t)_p$ and $\alpha = -(1/v)(\partial v/\partial p)_t$ are the volume expansivity and the isothermal compressibility, respectively.

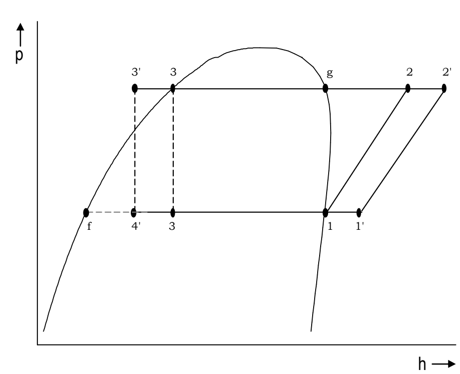

Figura 2. Thermodynamic representation of the refrigeration cycles under analysis in a p-h diagram

ISSN 2176-5480

Defining $\theta = \beta(t_c - t_e)$ and noting that $\varepsilon\theta << 1$ and also that dp=0 in case of constrained pressures, the specific volume ratio can be approximated as follows:

$$\frac{v_1'}{v_1} \approx 1 + \varepsilon\theta \tag{7}$$

Also noting that $h_3 - h_3' = \varepsilon c_{p,g}(t_c - t_e)$, and $h_1 - h_3 = h_{lv} - c_{p,f}(t_c - t_e)$, where h_{lv} is the refrigerant enthalpy of evaporation evaluated at p_e, eq. (5) can thus be rewritten as follows:

$$\frac{COP'}{COP} \approx \frac{1 + \varepsilon c_r \dfrac{\phi}{1-\phi}}{1 + \varepsilon\theta} \tag{8}$$

where $c_r = c_{p,g}/c_{p,f}$ is the specific heat ratio, and $\phi = c_{p,f}(t_c - t_e)/h_{lv}$ accounts for the available latent heat to produce additional refrigerating effect in comparison to the standard cycle. It should be noted that eq. (8) is the same one presented by Domanski et al. (1994), although written here in a dimensionless form. It shows that $COP' > COP$ if $c_r\,\phi/(1-\phi) > \theta$, independently of the heat exchanger effectiveness.

Figure 3 illustrates eq. (8) for evaporating pressures of -25°C and 7°C, and some refrigerants of current interest, such as R134a, R22, R290, R600a and R717. In this analysis, the condensing pressure was held fixed at 40°C. One should note that the first condition is typical of household refrigerators and freezers, whereas the second one is typical of air conditioning. In this work, all thermodynamic property calculations were performed by means of REFPROP 9.0 (Lemmon et al., 2010). It can be seen in Fig. 3 that the COP increases for refrigerants R134a, R290 and R600a, and decreases for refrigerants R22 and R717, thus confirming the trends reported in the literature (Gosney, 1982).

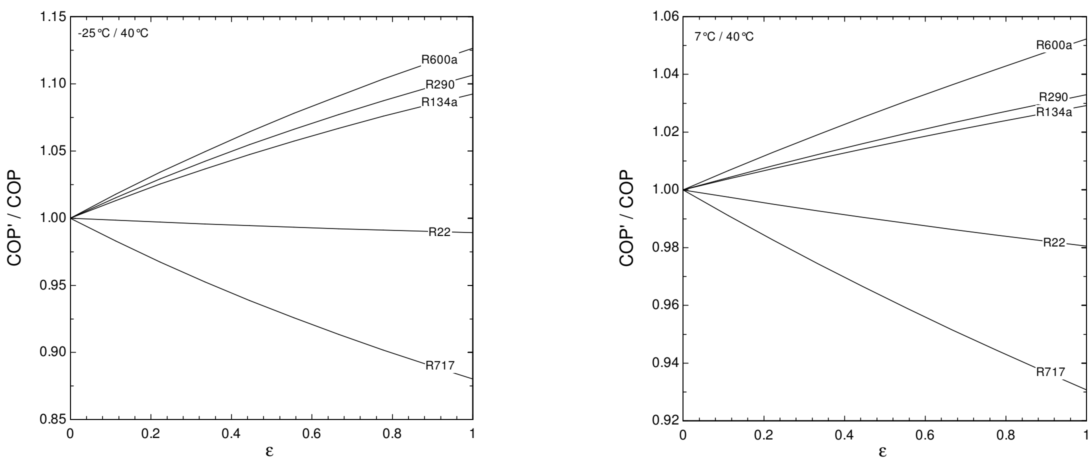

(a) (b)

Figure 3. COP variation in case of constrained pressures: (a) t_e=-25°C and (b) t_e=7°C (t_c=40°C)

Figure 4 summarizes the results for an internal heat exchanger with ε=1 for a wide evaporating temperature span. The condensing temperature was held fixed at 40°C. It shows that the COP'/COP trends are higher than 1.0 for refrigerants R134a, R290 and R600a for the whole range of evaporating temperatures, whereas the COP'/COP -values are lower than 1.0 for refrigerants R22 and R717. It can also be noted that the COP' experienced higher variations for the lower evaporating temperature, which is mainly due to its influence on ϕ, since there is more room for the specific refrigerating effect to increase in such a condition.

3. CONSTRAINED CAPACITY

So far, the exercise was restricted to cases where the working pressures are constrained, so that the cooling capacity is free to vary. In real refrigeration applications, however, the system is designed to accomplish a certain evaporator capacity, which is matched to the thermal loads by the control device. Therefore, a fairer evaluation of the advantages of the internal heat exchanger should assume the cooling capacity is constrained. In addition, noting that the condensing pressure remains fairly constant when an IHX is introduced into the cycle, as the condenser contains a larger amount of

ISSN 2176-5480

refrigerant than the evaporator, the following exercise was conducted assuming that $p'_c \approx p_c$, as well as the cooling capacity, $\dot{m}(h_1 - h_3) = \dot{m}'(h'_g - h'_3)$.

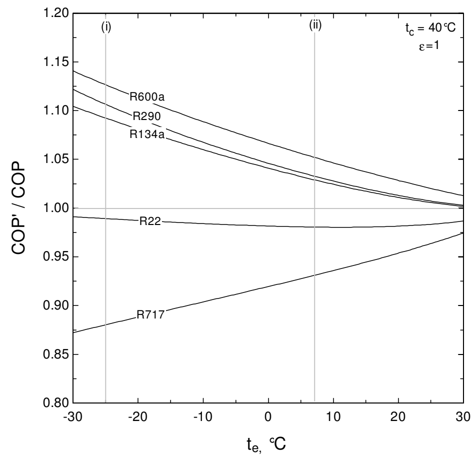

Figure 4. COP variation in case of constrained pressures for ε=1

Thus noting that $h'_g - h_1 \approx c_{p,g}(t'_e - t_e)$, one can show that the ratio between the mass flow rate of the standard cycle, $\dot{m}$, and the mass flow rate of the cycle using the internal heat exchanger, $\dot{m}'$, are calculated from

$$\frac{\dot{m}}{\dot{m}'} = 1 + c_r \frac{\phi}{1-\phi}\left(\frac{t'_1 - t_e}{t_c - t_e}\right) \tag{9}$$

Noting that $\dot{V} = \dot{V}'$, the mass flow rate ratio can be additionally calculated from

$$\frac{\dot{m}}{\dot{m}'} \approx \frac{\eta_v}{\eta'_v}\left[1 + \theta\left(\varepsilon + (1-\varepsilon)\frac{t'_e - t_e}{t_c - t_e}\right) - \alpha(p'_e - p_e)\right] \tag{10}$$

Assuming that $\eta_v \approx \eta'_v$, merging eq. (10) to eq. (9), and noting that $(1-\varepsilon)(t'_e - t_e) << t_c - t_e$, the following expression for the change experienced by the evaporating pressure can be derived,

$$\frac{p'_e}{p_e} \approx 1 - \frac{\varepsilon}{\alpha p_e}\left(c_r \frac{\phi}{1-\phi} - \theta\right) \tag{11}$$

Equation (11) shows that $p'_e < p_e$ if $c_r\,\phi/(1-\phi) > \theta$, which is quite the same criterion observed in eq. (8) for COP improvement in cases of constrained pressures. Therefore, in cases of constrained capacity, one can expect a decrease in the evaporating pressure for the very same conditions that lead to $COP' > COP$ in case of constrained pressures (see Fig. 3). Such a behavior is illustrated in Fig. 4, where one can see that the evaporating pressure decreases for refrigerants R134a, R290 and R600a, which have experienced COP augmentation when the working pressures were held constrained. The opposite behavior is observed for R22 and R717, which have undergone an evaporating pressure increase in case of constrained cooling capacity.

Figure 6 summarizes the results for ε=1, a wide evaporating temperature span, and a condensing temperature of 40°C. It can be noted that the trends of p'_e/p_e mirror those observed for COP'/COP, confirming that the factors which make the COP to increase in case of constrained pressures are the same that make the evaporating pressure to decrease in case of constrained capacity.

In addition, one can expect that the variation underwent by the evaporating pressure may improve or worsen the COP. Since both the cooling capacity and the compressor swept rate are constrained, the variation experienced by the coefficient of performance can be calculated from:

$$\frac{COP'}{COP} = \frac{w_v}{w'_v} \approx \frac{p_e}{p'_e}\left[\frac{(p_c/p_e)^{\frac{k-1}{k}} - 1}{(p_c/p'_e)^{\frac{k-1}{k}} - 1}\right] \tag{12}$$

ISSN 2176-5480

Gosney (1982) showed that there does exist a particular value of the evaporating pressure which maximizes the volumic work, w_v. Such a value is achieved making $\partial w_v / \partial p_e = 0$ in eq. (2) for a fixed condensing pressure, yielding

$$\frac{c}{1+c}(k-1)\left(\frac{p_c}{p_e^*}\right)^{\frac{1}{k}} + \left(\frac{p_c}{p_e^*}\right)^{\frac{k-1}{k}} - k = 0 \tag{13}$$

where p_e^* is the evaporating pressure value which maximizes wv for a fixed p_c.

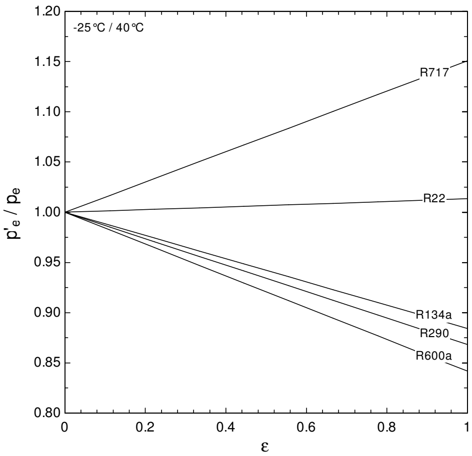

(a)

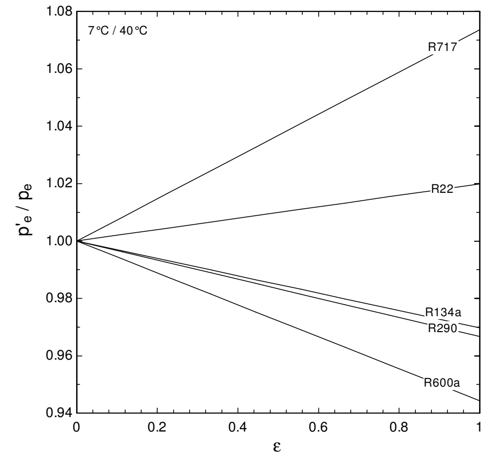

(b)

Figure 5. Evaporating pressure variation in case of constrained capacity: (a) t_e=-25°C and (b) t_e=7°C (t_c=40°C)

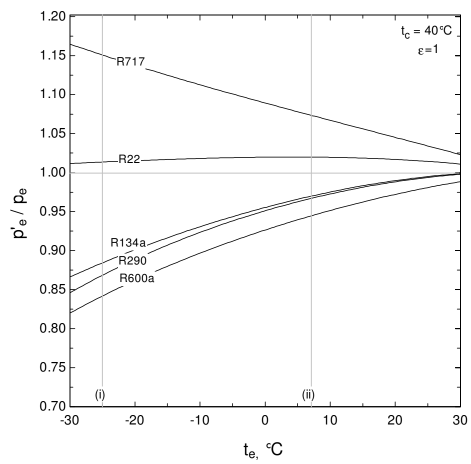

Figure 6. Evaporating pressure variation in case of constrained pressures for an IHX with ε=1

Figure 7 illustrates eq. (13) for different working fluids and a compressor with a 2%-clearance, where one can note that the volumic work may increase or decrease depending not only on the change experienced by the evaporating pressure (from p_e to p_e'), but also on what side of the maximum the evaporating pressure is. For instance, assume that $p_e' < p_e$. Thus, for LBP applications, $p_e < p_e^*$, so that $COP' > COP$. However, for HBP applications, $p_e > p_e^*$, then $COP' < COP$.

Figure 8 illustrates eq. (12). On one hand, for LBP applications (Fig. 8.a), the COP'/COP curves show the same trends observed for constrained pressures (Fig. 3.a), as the evaporating pressure, which is below the point of maxima (Fig. 7), diminishes for fluids R134a, R290 and R600a (Fig. 5.a), thus reducing the volumic work and increasing the COP. For refrigerants R22 and R717, however, $p_e' > p_e$ so that $COP' < COP$. For HBP applications, on the other hand, the trends are inverted (Fig. 8.b) when compared to those shown in Fig. 3.b, as a decrease in the evaporating pressure (as observed for refrigerants R134a, R290 and R600a in Fig. 5.b) augments the volumic work (the evaporating pressure is in the right-side of the maxima) thus reducing the COP. Refrigerants R22 and R717 experience a COP augmentation, as the evaporating pressure increases on the right-side of the maxima, thus reducing the volumic work.

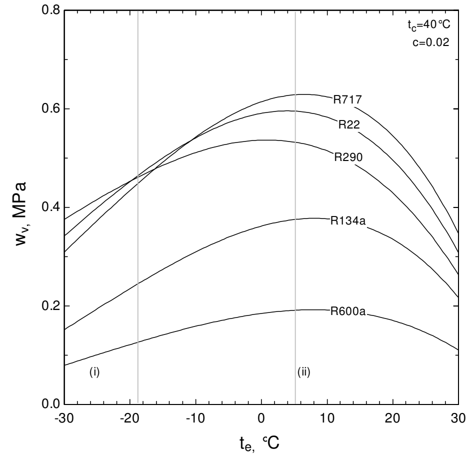

Figure 7. Mean effective pressure variation with the evaporating temperature

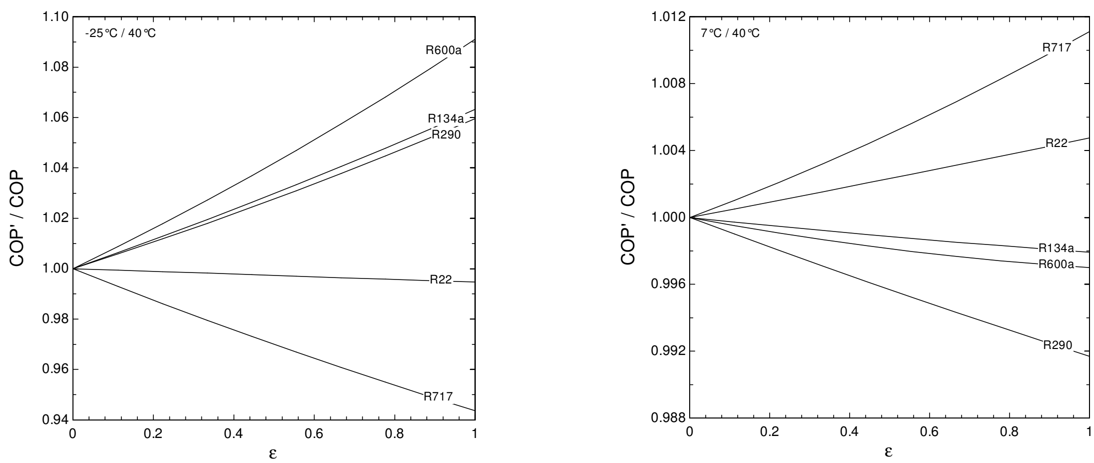

(a) (b)

Figure 8. COP variation in case of constrained capacity: (a) t_e=-25°C and (b) t_e=7°C (t_c=40°C)

Figure 9 summarizes the results for a wide evaporating temperature span for constrained capacity and ε=1. It can be seen clearly seen that the COP'/COP curves cross the 1.0-threshold for an evaporating temperature which corresponds to that which maximizes the volumic work, so that the $COP'/COP > 1$ for refrigerants R134a, R290 and R600a on the left-side, while $COP'/COP < 1$ for the same refrigerants on the right-side. In case of constrained working pressures (see Fig. 4) the COP'/COP trends are higher than 1.0 for refrigerants R134a, R290 and R600a for the whole range of p_e.

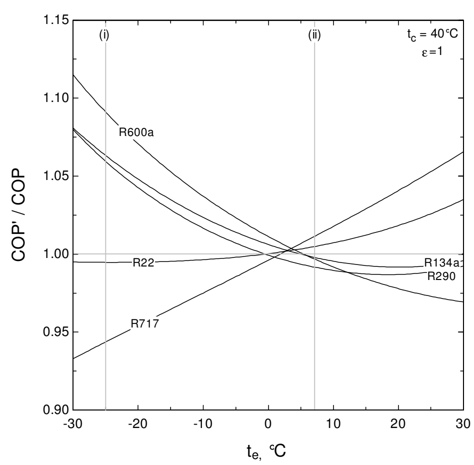

Figura 9. COP variation in case of constrained capacity for an IHX with ε=1

ISSN 2176-5480

4. FINAL REMARKS

The paper came up with a novel thermodynamic evaluation of the internal heat exchange in vapor compression refrigeration cycles. Differently from the previous studies, where the working pressures were considered to be the same for the standard and the modified cycle, the analyses carried out in this work considered the cooling capacity as a constraint, so that the evaporating pressure was free to float. It was observed that the COP may increase or not depending on the working pressures, the heat exchanger effectiveness, the specific heat ratio, the isentropic exponent, the isothermal compressibility, the volumetric expansivity, and the available latent heat to produce additional refrigerating effect. Therefore, the COP will increase either when the evaporating pressure decrease to values lower than that which maximizes the volumic work, or when the evaporating pressure increase to values higher than that which maximizes the volumic work. This explains why ammonia and R22, for instance, have shown performance reductions for LBP applications and performance improvements for HBP ones in case an internal heat exchanger is adopted. Such a behavior has not been identified in the textbook analyses where the workings pressures were held constrained.

5. ACKNOWLEDGMENTS

This study was carried out under the auspices of the Brazilian Government Agency CNPq (Grant No. 303789/2012-3).

6. REFERENCES

Domanski, P.A., Didion, D.A., Doyle, J.P., 1994, Evaluation of suction-line/liquid-line heat exchanger in the refrigeration cycle, Int. J. Refrigeration 17, 487-493

Gosney, W.B., 1982, Principles of refrigeration, Cambridge University Press, Cambridge, UK

Klein, S.A., Reindl, D.T., Brownell, K., 2000, Refrigeration system using liquid-suction heat exchangers, Int. J. Refrigeration 23, 588-596

Lemmon, E.W., Huber, M.L., McLinden, M.O., 2010, REFPROP: Reference Fluid Thermodynamic and Transport Properties, NIST Standard Reference Database 23 Version 9.0, Boulder-CO, USA

Stoecker, W.F., Jones, J.W., 1982, Refrigeration and Air Conditioning, McGraw-Hill, NY, USA

7. NOMENCLATURE

Roman

c	Compressor clearance, dimensionless
c_p	Specific heat at constant pressure, J/kgK
c_v	Specific heat at constant volume, J/kgK
c_r	Specific heat ratio, dimensionless
h	Specific enthalpy, J/kg
k	Isentropic exponent, dimensionless
p	Pressure, Pa
r	Pressure ratio, dimensionless
t	Temperature, K
v	Specific volume, m^3/kg
w_v	Mean effective pressure, Pa
q_v	Volumic refrigerating effect, Pa

Greek

α	Isothermal compressibility, 1/Pa
β	Volumetric expansivity, 1/K
ε	Heat exchanger effectiveness, dimensionless
ϕ	Available latent heat to produce additional refrigerating effect, dimensionless
θ	Refrigerant expansion factor, dimensionless

Subscripts

c	Condenser
e	Evaporator
f	Saturated liquid at the condensing temperature (Fig. 2)
g	Saturated vapor at the evaporating temperature (Fig. 2)
l	Saturated liquid
v	Saturated vapor